

A Global Tool for the Prediction of HF Surface Wave Propagation

Yannick Béniguel
IEEA
Courbevoie, France
beniguel@ieea.fr

Muriel Darces, Marc Hélier
Sorbonne Universités, UPMC Univ. Paris 06, UR2, L2E,
Paris, France

Alain Reineix
Xlim Institute, University of Limoges
Limoges, France

Abstract— This paper deals with the problem of HF surface wave radar. The goal is to integrate in a unique tool the antenna radiation and the propagation calculations in order to make the analysis consistent.

Keywords—HF, surface wave, MPIE, Near field to far field, propagation

I. INTRODUCTION

This paper addresses the problem of the surface wave (SW) radar¹. This kind of radar, usually operating in the HF band, has a growing interest in many applications, in particular for the survey of the coastal maritime sectors. Contrary to the sky waves, also radiated by a HF radar, the surface or ground waves decay as the square root of the distance to the source. As a result, and with a reasonable transmitted power, the signal can be propagated over hundreds of kilometers. Such a propagation mode complements the sky wave pattern of HF radars, which shows a blind zone up to the first ionosphere reflection distance.

To fully characterize the problem, both the antenna characterization and matching, the near field pattern and the propagation problem have been addressed. The antenna current distribution has been calculated using the integral equation technique [1]. Two numerical approaches to properly take the interface into account were developed concurrently. One advantage of the technique is to isolate the ground wave contribution and estimate the related radiated power. Once the current distribution is found, the near field and the far field pattern (including the ground wave contribution) can be obtained.

Another approach to the antenna problem consists in using a near field - far field transformation using measurements. An HF antenna is usually located above the ground and may reach dimensions up to 15 m height. As the ground interface is part

of the radiating structure, this puts some constraints on the measurement setup. Specific equipment is being studied for this purpose. The measurements will be performed using a 3D electric probe moved over a virtual cylindrical surface containing the antenna. The location of the sensor will be simultaneously recorded at each measurement point. The corresponding virtual magnetic currents distribution will allow calculating the field radiated at any point in the outer space. Those measurements will be tested firstly on a 1 GHz scale model and then applied to the actual HF antenna.

The ground wave propagation over an irregular, inhomogeneous terrain can be derived using the parabolic equation. The problem is an initial value problem with the ground wave field contribution acting as a driver, as the sky wave has no contribution in the interface plane. Two techniques were developed concurrently. The first one uses the classical split step technique while the second uses a finite difference scheme.

These different points are briefly commented in the following sections.

II. THE ANTENNA PROBLEM

As derived by Michalski [2], there are three different ways to write the Lorentz gauge relationship in order to meet the boundary conditions on the interface. Although equivalent from a theoretical point of view, his formulation C is the most convenient as regards its numerical implementation. This formulation has been used in the present development. With respect to the Electric Field Integral Equation (EFIE), the new equation, named Mixed Potential Integral Equation (MPIE), includes additional terms to take the Green's function modification into account.

The MPIE integral terms all involve the so-called Sommerfeld integrals. Two techniques can be used for their numerical evaluation, either the Phase Stationary Technique (PST) or the

¹ This study has been carried out in the frame of the PROPHETE project under funding of the French Research National Agency (ANR)

Complex Image Technique (CIT). These two techniques have been developed concurrently.

The phase stationary technique is the classical one. It consists in finding the steepest descent contour in the k_ρ complex plane. This contour has branch cuts as the function to integrate has branch points. The complex image technique [3-4] takes benefit from the easiness to consider images in a method of moments procedure. The aim of the calculation consists in representing the MPIE integral terms by a sum of terms, each of them being amenable to a Weyl like integral term. The integration is performed in the k_z complex plane. The integration contour is linear in this plane. Figure 1 shows a comparison of the E_z contribution of a vertical Electric Dipole (VED) obtained with the two techniques. The agreement is excellent.

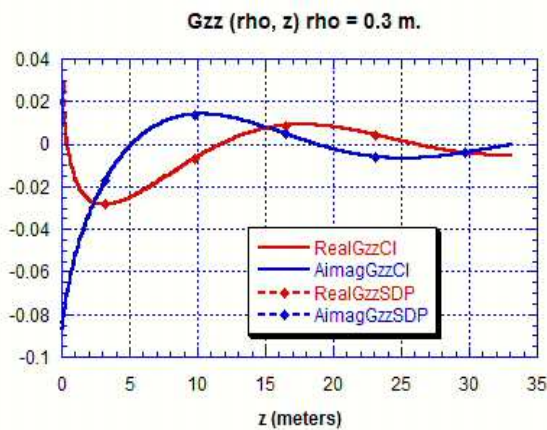


Figure 1 : Comparison of the electric field vertical component contributions due to a vertical dipole obtained with the phase stationary and the complex image technique

In addition to the contour contribution, the result shall integrate the poles contribution. The corresponding terms are the surface wave radiated by the HF antenna.

Again, the comparison between the two techniques has been performed. For the phase stationary technique, none of the poles are located inside the integration contour. However they are very close to it. As a result in order to make the calculation numerically tractable, it is necessary to remove their contribution in the integrand to get a regular function. It is subsequently reintroduced and calculated separately. This is the so-called modified saddle point calculation technique. For the complex image technique, all poles of the function should be included irrespective to their sign. They are considered by pairs. The comparison is shown in figure 2.

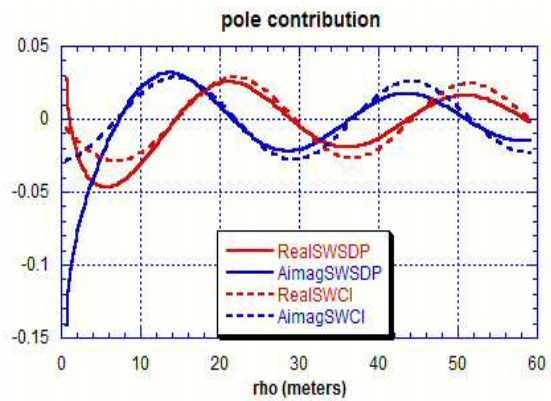


Figure 2 : Comparison of the electric field vertical component contributions due to the pole contribution for a vertical dipole obtained with the phase stationary and the complex image technique

Summary

For its implementation in a method of moments code, the Sommerfeld integral terms should give accurate results whatever the problem parameters such as the frequency, the distances and the electrical medium parameters are. To this respect, the complex image might be the most convenient technique, as accurate developments can be used for the critical values in the integration complex plane, namely when k_ρ and ρ tend to zero.

For the surface wave contribution, an analytical solution involving the error function, can be derived using the modified saddle point technique.

One example of results is presented hereafter using the software developed [2]. The case considered is a typical biconical antenna of 7 meters height placed on the ground (relative dielectric constant 15 and conductivity 0.05 S / m). The calculation provides the VSWR, the currents and the fields (near field, far field and ground wave). The antenna current distribution is shown in figure 3.

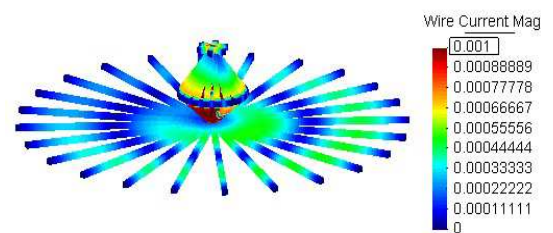


Figure 3 : Currents distribution on the HF antenna

Figure 4 shows the near field pattern on a cylindrical surface containing the antenna. The major contribution comes from the ground wave. It decreases very rapidly with the altitude and as the inverse of the square root of the radial distance to the antenna for an observation point at the air ground interface.

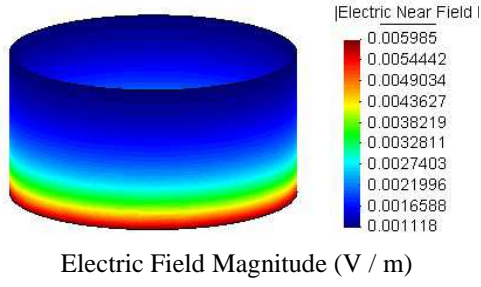


Figure 4 : The near field radiated by the antenna on a cylindrical surface of radius 100 meters with the antenna at its base centre.

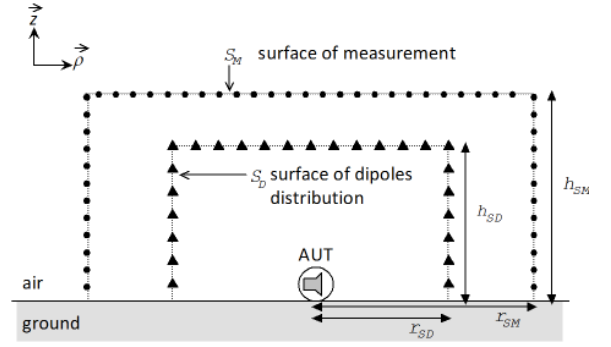


Figure 5: Geometry corresponding to the method.

Equations (1) can be solved by inversion of the matrix $\begin{bmatrix} \mathbf{D}_E \\ \mathbf{D}_H \end{bmatrix}$ in order to compute the vector \mathbf{P}_{SD} . The accuracy of the inversion depends on the actual number of dipoles contributing to the radiation. More precisely, the idea is to unselect the dipoles that have a non-significant contribution to the total field. To achieve that goal, this inversion is carried out by applying the singular value decomposition (SVD) to the matrix $\begin{bmatrix} \mathbf{D}_E \\ \mathbf{D}_H \end{bmatrix}$ associated with a threshold power criterion (Fig. 6).

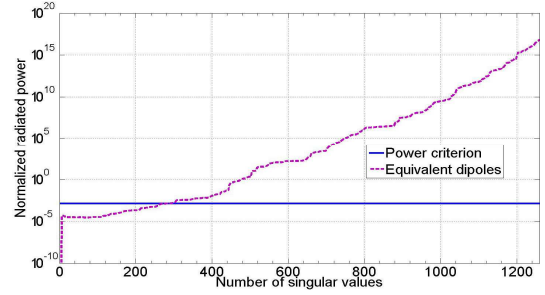


Fig. 6 Power radiated by the equivalent dipoles vs. singular values.

This criterion is linked to the total power radiated by the AUT, in the near field zone, and is calculated from the measurement of the electromagnetic field on surface S_M . Then, the singular value matrix is scanned and truncated by decreasing order until the corresponding calculated power reaches this power criterion. Once the vector \mathbf{P}_{SD} is determined, the electric far field can be easily computed. In order to perform the SVD, we need to know both the electric and magnetic fields. However, to avoid measuring the magnetic field, it is possible to approximate it, based on the plane wave assumption, and still apply the power criterion.

B. Results

Let us consider a quarter-wave monopole working at 10 MHz and located above moist soil ($\epsilon_r = 13$ and $\sigma = 0.05 \text{ S.m}^{-1}$). The near-field data are obtained from CST MWS. Fig. 7 shows the amplitude and phase of the electric field extracted from CST MWS and the one calculated thanks to the NF/FF transformation. As we can see, the electric near field is well reconstituted.

III. NEAR-FIELD TO FAR-FIELD (NF/FF) TRANSFORMATION IN THE HF BAND

The proposed method is based on a source identification assuming that the antenna under test (AUT) can be replaced by a set of equivalent dipoles radiating the same far-field as the AUT. This approach, based on the equivalence principle, has been already described by several authors [3]. Nevertheless, the innovative point brought by this new method is the use, as dipole's radiation functions, of the analytic formulations developed by Norton and extended by Bannister [4] to the very near field zone. These formulations comprise the sky wave, which is the sum of the direct and reflected waves, as well as the surface wave contribution of the electromagnetic field radiated by each elementary dipole.

A. Description of the method

Consider an AUT located at the plane horizontal interface between air and real ground. The components of the electromagnetic field are measured in the near-field zone (in order to acquire the surface wave) on a virtual surface S_M surrounding the AUT (Fig. 5). The number of measured points is N_M . Consider now a second virtual surface S_D , included inside the surface S_M (Fig. 5). The number of mesh points is N_D . At each point, three elementary electric dipoles are arranged in order to form an orthogonal basis aligned with the cylindrical basis vectors. The method states that, at each point of the surface S_M , the electromagnetic field, is equal to the sum of all the contributions coming from each of the $3N_D$ dipoles distributed over surface S_D . This leads to the following matrix equation:

$$\begin{bmatrix} \mathbf{D}_E \\ \mathbf{D}_H \end{bmatrix} [\mathbf{P}_{SD}] = \begin{bmatrix} \mathbf{E}_{S_M} \\ \mathbf{H}_{S_M} \end{bmatrix} \quad (1)$$

where \mathbf{E}_{S_M} and \mathbf{H}_{S_M} denote the electric and magnetic vectors of size $3N_M$, measured at each point on the surface S_M . \mathbf{D}_E and \mathbf{D}_H are respectively the electric and magnetic radiation matrices (issued from the Norton/Bannister formulations), of size $3N_M \times 3N_D$, concerning the $3N_D$ electric (horizontal and vertical) dipoles located at each point of the surface S_D . \mathbf{P}_{SD} is the unknown vector, of size $3N_D$, containing the electric moments of the previous dipoles.

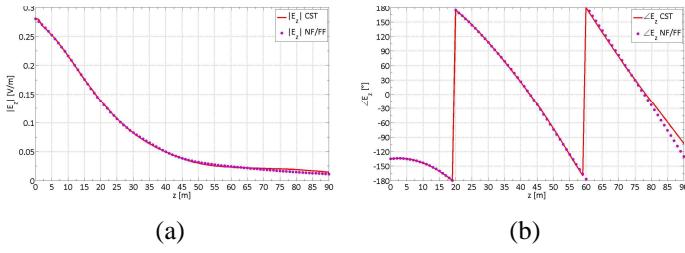


Fig. 7. Electric near field over a generating line of the cylinder: (a) magnitude, (b) phase.

Now, we discuss about the far field results. Unfortunately, CST MWS does not take into account the surface wave in the far field zone, but the results obtained by means of the SVD method have already been compared to the results obtained with NEC/SOMNEC [5-6] and are satisfactory. E_θ is the far field component of the electric field determined after a SVD considering both electric and magnetic near fields, and E_θ' is the far field component of the electric field determined after the SVD, from the electric near field only. At a distance of 10λ from the antenna, we can see in Fig. 8 that the surface wave ($\theta \approx 90^\circ$) is predominant [6]. But at 100λ from the antenna, the sky wave is predominant, and reaches its maximum magnitude at $\theta \approx 70^\circ$ (Fig. 9).

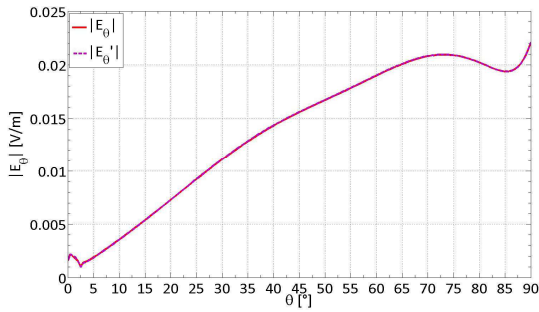


Fig. 8. Radiated electric field at 10λ .

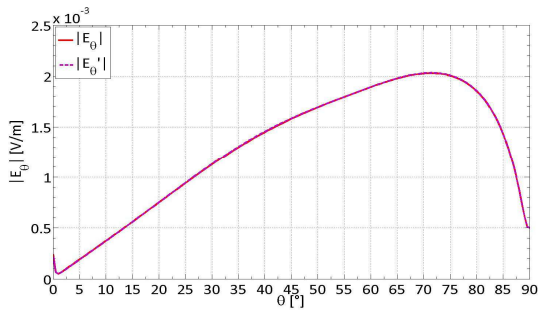


Fig. 9. Radiated electric field at 100λ .

The two radiation patterns depicted in Fig. 8 and Fig. 9 have a shape which evolves with respect to the distance as expected, and it can be concluded that the SVD method is accurate enough in order to compute the radiated far field thanks to the sampled data of the electric near field, only.

IV. PROPAGATION

Two techniques have been developed to address the propagation problem. The first one uses a multiple phase screen technique while the second one uses a finite difference technique. This double approach was implemented in order to allow cross checking of the results. The main points of each one of the two techniques are commented hereafter.

The two techniques are based on a resolution of the parabolic equation. This equation is obtained from the Helmholtz equation, assuming that the field variation along the line of sight (LOS) is weak as compared to its variation in the plane transverse to this direction. This hypothesis, referred as the paraxial approximation, is only valid for angles with the LOS lower than about 15° . This equation was used in the two approaches developed. The main features, namely the source term, the boundary conditions and the algorithm are presented for the two techniques. In the two cases the algorithm is a 2D algorithm, marching on in space from the source location to a given observation point. The field is calculated on vertical lines with respect to the mean tangent plane.

The initial field, on the first vertical, is deduced from the antenna analysis problem. It shall be noticed that only the surface wave shall be considered as it can be demonstrated that the sky wave has no contribution in the air - ground interface plane. The antenna analysis integral equation technique allows isolating this contribution. In principle either the SW near field radiated by the antenna or the far field expression of the SW can be used as inputs, in this last case using a Fourier inverse transformation to get the equivalent aperture source. The near field calculation is however found to be the most accurate as the SW far field involves the large argument approximation of the Hankel function, this condition is not obviously met in the HF domain.

The multiple phase screen technique takes advantage of the fact that the parabolic equation reduces to an ordinary differential equation when using a Fourier transformation from the space domain to the kz domain where kz is the vertical component of the wave number. The algorithm alternates consequently two calculations at each space step : the Fourier transform calculation and the differential equation calculation. The first one allows considering the scattering effects and the second one the field modification due to the propagation along the LOS. There remains the problem of the boundary conditions. On the upper altitude of the space domain, an absorbing boundary condition shall be implemented as no field shall be reflected. This is done using an apodisation function. At the air - ground interface, the Leontovich conditions are implemented. Following Dockery & Kraig [7], a complementary function has been used allowing to implicitly meet the boundary conditions. This is facilitated by using sine Fourier transforms. The overall algorithm is very efficient allowing considering arbitrary terrain profiles and ground impedance discontinuities. The CPU time is very small, typically a few tenths of seconds for a wave propagation over 300 kilometers.

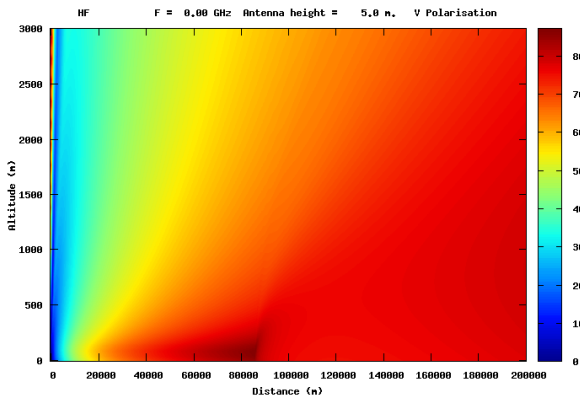


Figure 10 : HF propagation; impedance discontinuity at 86 km

Figure 10 shows an example of the field attenuation in a 2D window calculated using the MPS technique. The profile has an impedance discontinuity 86 km away from the source. After this distance the propagation, which was previously over land, is over sea. The field attenuation at the air – ground interface is shown on Figure 15.

The finite difference technique on the other hand uses a centre finite difference scheme as shown on Figure 10. In this case, the center point is located between two vertical lines. This scheme leads to a tridiagonal matrix.

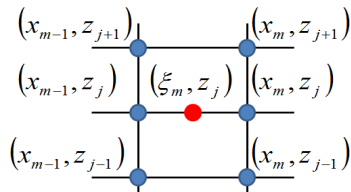


Figure 10 : Finite differences scheme

The upper boundary condition is an adaptation of the PML first introduced by Berenger [8]. An efficient way to introduce the PML in the FD grid is to use stretched coordinates [9] in the vertical direction. Such an approach allows deriving the equation to be solved into the PML region. To test the validity of the implementation, a 10 layers PML medium and a parabolic profile of conductivity were considered. A Gaussian bunch of rays is launched with a tilted angle in the direction of the PML (upper boundary direction) chosen according to the narrow angle parabolic equation limitation (about 10 degrees). The result plot on Figure 11 shows that there is no reflection on the upper boundary.

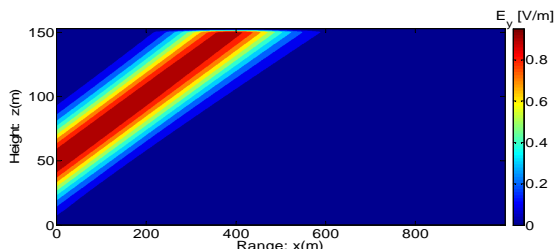


Figure 11: Simulation of a beam launched towards a PML boundary condition.

The lower boundary condition implements, as in the MPS technique, the Leontovich condition. In addition the ground surface roughness can be super imposed on the profile. Two techniques have been developed to do this. The first one consists in the generation of a white noise, making a Fourier transform, filtering and coming back in the spatial domain. The characteristics of the filter have to be chosen in agreement with some statistical parameters of the real ground: correlation length and root square means of the height. Figure 12 shows two realizations with two different correlation functions.

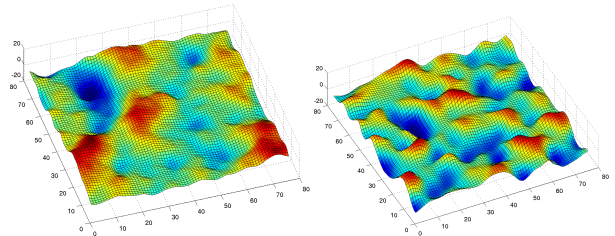


Figure 12 : Results of the statistical methods: Exponential white noise filtering (left panel), Gaussian white noise filtering (right panel)

The second technique uses a fractal model. The Diamond square approach has been adapted to model the surface. The terrain roughness can be controlled by means of a given parameter, named h as shown on Figure 13

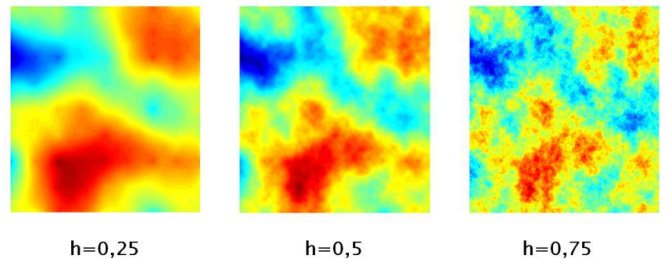


Figure 13 : Surface roughness realization using a fractal technique

Figure 14 shows an example of propagation in a 2D window using a profile extracted from a fractal surface realization.

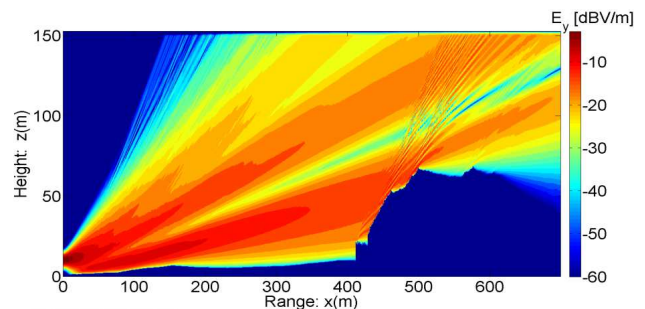


Figure 14 : Propagation over an irregular surface

Comparison of results obtained with the MPS and the FD techniques

The consistency between the results provided by the two approaches have been cross checked with respect to a classical problem, namely the one exhibiting the Millington effect showing a recovery of the field strength after crossing a discontinuity (cf Figure 15). The agreement between the results is excellent.

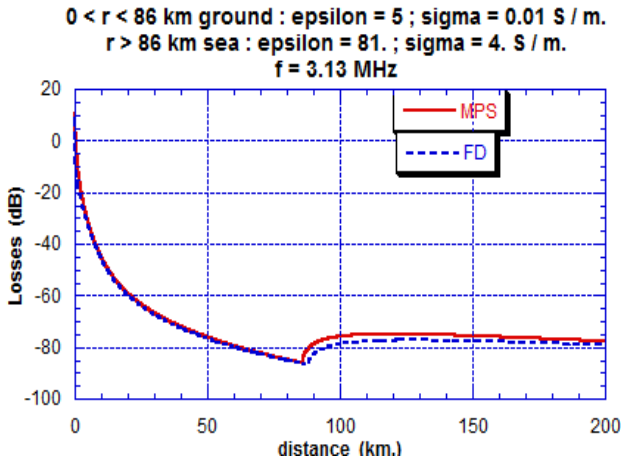


Figure 15 : Field propagation on a terrain with an impedance discontinuity

V. DOPPLER EFFECT / PROPAGATION OVER THE SEA

One of the study objectives was to model the propagation over the sea. As the sea models are based on physical considerations, such a model (JONSWAP) based on the directional spectrum of the sea has been included in the software. It strongly depends on the wind direction and strength (Beaufort). It is able to represent the effect of the sea deformation due to the gravity waves. An obtained realization of the sea surface is shown on Figure 16.

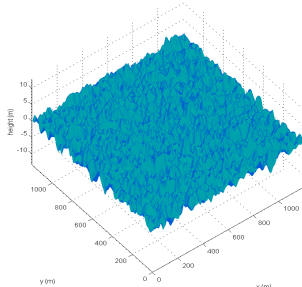


Figure 16 : Sea surface modelling

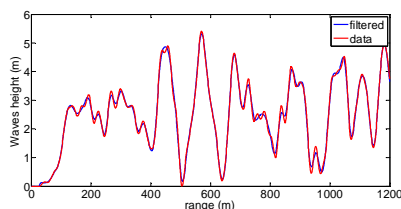


Figure 17 : Sea profile

To perform the Doppler calculation, a profile is extracted from the realization shown on Figure 17. This profile, shown on Figure 18 is introduced in the parabolic equation software. Different realizations are considered at successive times. The backscattered field is then computed at the operating frequency. The integration on a long observation time of the moving sea gives the Doppler spectrum computed by expression :

$$\mathcal{S}(f) = \left| \int_0^{T_{obs}} E_s(t) e^{-j2\pi ft} dt \right|^2 \quad (2)$$

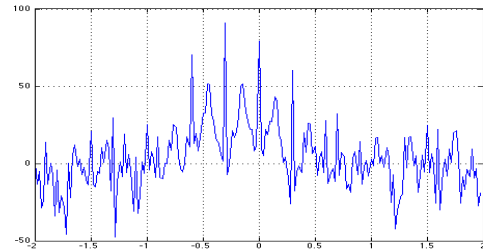


Figure 18 : Observed spectrum for the following set of input data : $f=15$ MHz, $\lambda_s=10$ m, $dt=0.25$ s, $T_{obs}=50$ s, $u=3$ m/s
 $f_d=0.3$ Hz

This calculation provides the Doppler spectrum components as expected.

VI. CONCLUSION

Many innovative points have been considered in this study aiming to develop a global tool allowing addressing the antenna plus surface wave propagation problem. At each step of the study two calculations and / or measurements techniques were developed concurrently giving full confidence in the obtained results.

References

- [1] Michalski K., D. Zheng, "Electromagnetic Scattering and Radiation by Surfaces of Arbitrary Shape in Layered Media, Part I: Theory", IEEE AP, Vol 38, N° 3, 1990.
- [2] <http://www.ieea.fr/fr/logiciels/icare-mom.html>
- [3] F. Fan, F. Schlagenhafer, "Source identification and correlation between near field-far field tolerances when applying a genetic algorithm", International Symposium on Electromagnetic Compatibility (EMC), pp.1-6, Sept. 2008.
- [4] P. Bannister, "The quasi-near fields of dipole antennas", IEEE Transactions on Antennas and Propagation, vol.15, no.5, pp. 618- 626, Sept 1967
- [5] N. Payet, M. Darces, J. L. Montagnon and M. Hélier, "Near Field to Far Field Transformation by using Equivalent Sources in HF Band", 15th International Symposium on Antenna Technology and Applied Electromagnetics (ANTEM), pp. 1-4, June 2012.
- [6] C. Djoma, M. Darces, M. Hélier, "Prediction of Sky and Surface Wave Radiation of a Wideband HF Antenna", IEEE Antennas and Wireless Propagation Letters, doi: 10.1109/LAWP.2015.2391295.
- [7] G.D. Dockery, J.R. Kutler, "An improved impedance boundary algorithm for Fourier split step solutions of the parabolic wave equation", IEEE Trans. Antennas and Propagation, vol. 44, pp. 1592 – 1599, 1996
- [8] J.-P. Béranger, "A perfectly matched layer for the absorption of electromagnetic waves," J. Comput. Phys., vol. 114, no. 1, pp. 185–200, 1994
- [9] W. C. Chew and W. H. Weedon, "A 3d perfectly matched medium from modified Maxwell's equations with stretched coordinates," Microwave and Optical Tech. Lett., vol. 7, no. 13, pp. 599–604, 1994

